IEEE Access
Multidisciplinary ⋮ Rapid Review ⋮ Open Access Journal

Received 25 December 2023, accepted 31 March 2024, date of publication 8 April 2024, date of current version 15 April 2024.

Digital Object Identifier 10.1109/ACCESS.2024.3385771

RESEARCH ARTICLE

Mitigating the Inrush Current of V/V Transformers Using Railway Conditioners

AMIR AGHAZADEH[1], (Student Member, IEEE), EHSAN HAJIPOUR[2], (Member, IEEE), KANG LI[1], (Senior Member, IEEE), AND SADEGH AZIZI[1], (Senior Member, IEEE)

[1] School of Electronic and Electrical Engineering, University of Leeds, LS2 9JT Leeds, U.K.
[2]Center of Excellence in Power System Management and Control, Department of Electrical Engineering, Sharif University of Technology, Tehran 11365-11155, Iran

Corresponding author: Amir Aghazadeh (elaagh@leeds.ac.uk)

ABSTRACT Inrush current is high-magnitude current drawn by power transformers upon energization. The severity of inrush current depends on factors such as the transformer's residual flux and the voltage phase angle at the energization instant. This paper proposes a flux matching method for the energization of V/V traction transformers to mitigate inrush current. This is achieved by adjusting the residual flux of the core to an appropriate reference value and then obtaining the proper energization instant. To this end, the method only requires knowledge of nominal voltage and excitation current, eliminating the need to acquire transformer's parameters/design information. The railway power conditioner, typically present at the low voltage side of the V/V transformer, is used as a current source to inject sinusoidal current into the transformer windings before its energization. The reference residual flux is calculated based on the circuit breaker operating characteristics. The energization instant is determined such that the adjusted flux density matches the steady-state flux expected with respect to the applied voltage. The proposed method is validated by conducting over 14,000 simulations under different conditions using PSCAD/EMTDC. The method is also implemented and successfully tested on a laboratory-scale test rig, which verifies its effectiveness in more realistic conditions.

INDEX TERMS Inrush current, flux density, excitation current, railway power conditioners, V/V transformers.

I. INTRODUCTION

High-speed electric trains have been receiving increasing attention to meet the increasing transportation demand thanks to their reliable and environmentally friendly performance. Power quality is of high importance to traction systems that power high-speed electric trains. The energization of a traction power transformer, similar to any other power transformers, may result in the flow of high-magnitude excitation current (known as inrush current) [1]. This stems from the ferromagnetic characteristics of transformers' magnetic core [2].

The associate editor coordinating the review of this manuscript and approving it for publication was Jesus Felez.

Inrush current typically contains a significant DC component and is rich in harmonics. These undesirable features of inrush current cause power quality degradation, malfunction of protective relays, mechanical stress to transformers, and unnecessary expenditure of their lifetime [3]. Both inrush and short-circuit fault currents can result in a significant discrepancy between the currents of primary and secondary windings. As such, the presence of inrush current can mislead the differential protection to unnecessarily interrupt the circuit. This will prolong the transformer's energization process and increase the number of times the transformer windings must withstand undesirable axial and radial forces.

Existing methods for dealing with inrush current can be divided into passive and active categories. The working

principle of the first category [4], [5], [6], as the dominant practice, is distinguishing between the presence of inrush and short-circuit fault currents to interrupt power to the transformer in the latter case. When a transformer is energized, passive methods let the inrush current flow and vanish naturally after several power-frequency cycles. The techniques proposed in [4], [5], and [6] can improve the ability to distinguish between inrush and fault currents. Nevertheless, passive methods are essentially aimed at limiting the number of required energization attempts to a minimum of one. Thus, these methods still present the transformer with over-currents, thereby resulting in a needless reduction in the transformer's lifespan following each energization attempt [3].

Methods of the active category are aimed at the removal of inrush current, thus minimizing the damaging forces on the transformer while reducing the pressure on the protection system [7], [8], [9], [10], [11], [12], [13], [14], [15], [16], [17], [18], [19], [20], [21], [22], [23], [24], [25], [26]. References suggest special transformer designs to alleviate inrush current. Another popular approach is increasing the transformer's stiffness against inrush current by temporarily inserting passive resistors [9], [10], [11] or power electronics-based current limiters [12], [13], [14], [15] into the circuit. These methods rely on complicated design processes and/or control mechanisms to minimize inrush current, which increases manufacturing and maintenance costs.

The term ''residual flux'' refers to the magnetic flux that remains trapped within a transformer's core once the transformer has been de-energized [27]. ''Prospective flux'' refers to the expected flux within the core of the transformer at the moment of energization, assuming there is no transient response and the transformer has already reached a steady-state. A difference between the residual and prospective fluxes causes inrush current to flow upon transformer energization [16]. This paper uses the term ''flux matching'' to refer to the process of eliminating the difference between residual and prospective fluxes to mitigate inrush current. Flux matching methods fall under the active category and normally involve an initial stage of flux adjustment/estimation and a final stage of controlled switching.

Flux matching methods proposed in [16], [17], and [18] formulate the energization instant as a function of residual flux density, and the circuit breaker (CB) operating characteristics discussed in [19], [20], and [21]. A technique is proposed in [18] that estimates the residual flux as the integral of the voltage across windings during CB tripping. The method presented in [22] can estimate the residual flux of single-phase transformers using DC excitation. Residual flux estimation using magnetic sensors and a finite-element model is proposed in [28]. In general, the inaccuracy of measurements taken in transient conditions undermines the validity of residual flux estimation methods. As another major problem, these methods disregard the fact that the core's residual flux might change with time following the transformer's de-energization [23].

Circumventing difficulties associated with reliable estimation of residual flux [23], a flux adjustment method is proposed in [24], [25], and [26] to adjust the core's flux to a pre-determined value. This is accomplished by connecting the transformer to a capacitor of appropriate size. To determine the size of the capacitor needed, particular design information about the transformer is necessary. This information, however, may be unreliable due to transformer aging or even unavailable for not having been provided by the transformer's manufacturer. In the controlled switching stage, [24], [25], [26] assume that CBs are ideal and can let current flow immediately after the reception of a closing command. Nevertheless, disregarding CB operating characteristics can highly reduce the effectiveness of methods in mitigating inrush current or even make them counterproductive. The demagnetizing technique proposed in [29] applies a DC voltage source with alternating polarity to remove the residual flux. This technique is not ideal for energizing a single power transformer [23], [30].

This paper proposes a flux matching method for mitigating the inrush current of V/V transformers widely employed in traction systems [31]. The proposed method is able to adjust the transformer's residual flux density to any value within the feasible range, contrary to existing methods. This is achieved by injecting appropriate current into the V/V transformer using a railway power conditioner. The only must-know parameter is the transformer's nominal excitation current, and other information will be obtained throughout the flux adjustment process. Not relying on transformer design information removes a significant source of difficulties/uncertainties. Performance evaluation is carried out in PSCAD/EMTDC and on a laboratory-scale V/V transformer to demonstrate the effectiveness of the proposed method. Results confirm the method's ability to mitigate inrush current and its superiority over existing methods under various conditions.

II. INRUSH CURRENT UPON TRANSFORMER ENERGIZATION

Let B and H denote the flux density of a ferromagnetic core and the magnetic field strength, respectively. The relationship between B and H is nonlinear and defined by a hysteresis loop (also referred to as the B-H curve). The instantaneous value of B depends not only on the present value of H but also on in what direction H has changed in the past. Let B_r denote the residual flux density of the core. The term steady-state flux density is used to denote the flux density of the core a long time after a sinusoidal voltage is applied to the transformer winding. Denoted by B_p, the prospective flux is defined as the instantaneous value of the steady-state flux density, at the instant of transformer energization [17], [18]. The reason for the flow of inrush current upon transformer energization is a difference between B_r and B_p.

To detail how a difference between B_r and B_p results in inrush current, a single-phase transformer is considered and energized at $t = t_e$. To this end, let us assume that the nominal

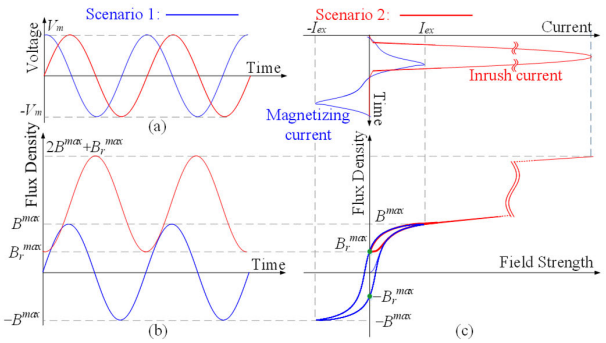

FIGURE 1. Transformer's (a) winding voltage, (b) core's flux density, (c) *B* - *H* curve and excitation current following Scenarios 1 and 2.

voltage $v(t) = V_m \cos(\omega t + \varphi_0)$ is applied to the primary winding of the transformer, while its secondary winding is open-circuited. Using Faraday's law, one can derive the flux density of the core as a function of time as below [32]

$$B(t) = \frac{1}{NA}\int_{t_e}^{t} V_m \cos(\omega t + \varphi_0)\, dt + B_r$$
$$= \underbrace{B^{max}\sin(\omega t + \varphi_0)}_{\text{steady-state component}} \underbrace{-\overbrace{B^{max}\sin(\omega t_e + \varphi_0)}^{B_p} + B_r}_{\text{DC component}} \quad (1)$$

where $N$and A are the number of winding turns and the core's cross-section area, respectively. It can be confirmed that $B^{max} = V_m/NA\omega$ will be the maximum flux density in normal operation, i.e., the RMS peak value of the steady-state flux density of the core. In (1), the steady-state component is sinusoidal while B_r and B_p are constant terms causing a DC shift in the core's flux density. The DC component would not exist provided that $B_p = B_r$.

To study how the presence of a DC component in the flux density impacts the energization of a single-phase transformer, two different scenarios are defined and explored. Without loss of generality, the time reference is chosen such that $\varphi_0 = 0°$. In Scenario 1, the residual flux density is assumed to be zero, i.e., $B_r = 0$, and the transformer is energized at a voltage peak. In Scenario 2, B_r is equal to B_r^{max})which is the maximum residual flux density possible). In this scenario, the transformer is energized at the rising zero-crossing of the voltage waveform. Fig. 1(a) demonstrates that the nominal voltage $v(t) = V_m \cos(\omega t + \varphi_0)$ is applied to the primary winding at $t = 0$while the secondary winding is open-circuited. The waveforms corresponding to Scenarios 1 and 2 are shown in blue and red, respectively. As can be seen, $\varphi_0$is equal to 0° in Scenario 1, and equal to −90° in Scenario 2. It can be understood from (1) that B_p is a function of the time-integral of voltage applied to the winding. It follows from (1) that the core flux contains only a sinusoidal oscillating term in Scenario 1 as $B_p = B_r = 0$. In Scenario 2, however, (1) consists of constant and sinusoidal oscillating components since $B_p \neq B_r$.

Fig. 1(b) shows the core's flux density under Scenarios 1 and 2. The *B-H* curve and excitation current corresponding to Scenarios 1 and 2 are also shown in Fig. 1(c), where the double tilde on a curve signifies the long continuation of the curve that could not be easily fitted in the figure. The flux density in Scenario 1 is a sinusoidal waveform (shown in blue) that starts from $B_r = 0$ with no DC shift and varies within the range $[-B^{max}, B^{max}]$. These two values refer to the knee points on the *B-H* curve and mark the bounds of the normal operating region of the core [32]. When the transformer is energized as per Scenario 2, the core's flux density begins to increase from an initial value of $B_r = B_r^{max}$. In this scenario, the difference between B_r and B_p leads to a DC shift ($B^{max} + B_r^{max}$) in the generated flux density in the core. Contrary to the blue curve of Scenario 1 where B varies between $-B^{max}$ to B^{max}, the red curve of Scenario 2 varies between B_r^{max} and $2B^{max} + B_r^{max}$ due to the DC shift. As a result, the transformer is driven into the deep saturation region leading to high H.

Indeed, Scenario 1 is the best energization scenario as it only draws the nominal excitation current. In Scenario 2, as the worst-case energization scenario, the current drawn is far greater than the excitation current due to the core saturation. The fact that $B_p = B_r = 0$ in Scenario 1 ensures that the flux density in the core does not exceed $\pm B^{max}$, thus a normal excitation current. A non-zero B_r results in a DC shift in the core's flux density thus deriving part of the magnetization into the saturation region. This is a region where the relationship between B and H is nonlinear and H increases significantly with a small change in B. Therefore, a high-magnitude asymmetric inrush current will result, which damps out only after several power-frequency cycles (thanks to the resistive nature of the system) [33].

III. FLUX MATCHING: CONCEPT AND CHALLENGES

In the context of transformers' energization, flux matching refers to the process of minimizing the difference between the residual and prospective fluxes (B_r and B_p), thus mitigating inrush current. The first stage of this process requires the estimation of the core's residual flux density or adjusting it to a certain value. This will be followed by the controlled switching stage, which energizes the transformer at an appropriate instant. Between residual flux estimation and adjustment, the latter may be preferred for two reasons. One is the inaccuracy of measurements over the transient period started by a disturbance and terminated by the transformer de-energization [34]. The second reason is that stray or shunt capacitances can discharge through a transformer and reduce the residual flux, which is known as ringdown transient. This phenomenon is a natural resonant response of the circuit formed by the transformer's main inductance and capacitances after transformer de-energization complicating the estimation of residual flux [23].

References [24] and [25] present a viable approach for flux adjustment before the controlled switching of CBs. To briefly explain this approach, let B_r^{ad} denote the adjusted residual

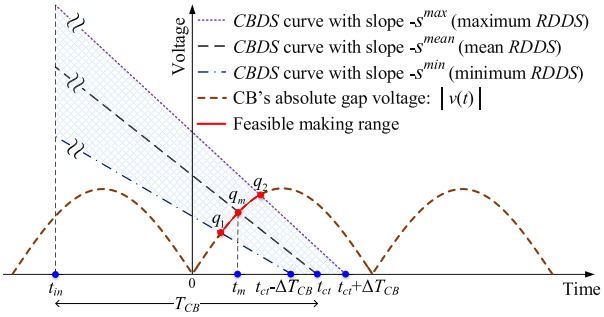

FIGURE 2. CB operating characteristics considering mechanical and *RDDS* scatter.

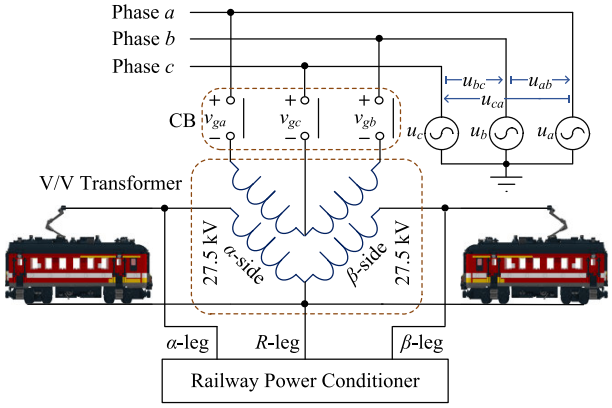

FIGURE 3. V/V traction transformer equipped with a railway power conditioner.

flux density of the core, where the superscript "*ad*" is used to differentiate this value from the core's initial flux density, i.e., B_r. In the flux adjustment stage, B_r is adjusted to $\pm B_r^{max}$ by discharging a capacitor into the transformer's winding. A controlled switching stage is then implemented to minimize $B_p - B_r^{ad}$. To be able to match the prospective fluxes corresponding to $\pm B_r^{max}$, the transformer must be energized at a few specific energization instants, which may or may not be achievable considering the limitations and operating characteristics of the CB. Indeed, the limitations of CBs render a range of making instants, thus a range of prospective fluxes, impossible to achieve. The energization of transformers using the methods of [24] and [25] can even be counterproductive, in practice, due to the significant difference between B_r^{ad} and B_p, as will be shown in the simulation section.

The residual flux B_r^{ad} can, in principle, be only adjusted to values within the feasible range $[B_r^{max}, B_r^{max}]$. This means the prospective flux within the ranges $(B_r^{max}, B^{max}]$ and $[B^{max}, B_r^{max})$ must be avoided, if inrush current is to be mitigated. It is also crucial to note that the uncertainty involved in the closing operation of CBs makes it impossible to determine the exact instant at which the transformer gets energized. Thus, an effective flux matching method for mitigating the inrush current of transformers needs to

- Account for the CB's operating characteristics and associated limitations/uncertainties.
- Be able to adjust the residual flux density to any value within the corresponding feasible range.
- Require little to no knowledge about the transformer's parameters and design information.

The rest of this section provides a basic explanation of the CB closing operation in order to highlight the importance of the first feature. The second feature helps minimize the consequences of the non-ideality of CBs. The rationale for the third feature is self-evident. Even when such information is available, it cannot necessarily be trusted due to environmental conditions and transformer aging.

Fig. 2 shows the closing operation of a CB, which starts at t_{in}. The closing operation continues until a metal-to-metal contact takes place between the CB poles, which is referred to as the instant of contact touch (t_{ct}). The time interval from the initiation of the closing operation to the instant of contact touch is known as the closing time, i.e., T_{CB}. The closing time depends on the velocity of the moving contact on its travel towards the fixed contact over the course of the CB closing operation. The continuous reduction in the distance between the CB fixed and moving contacts reduces the CB dielectric strength (*CBDS*) at the rate of decrease of dielectric strength (*RDDS*). From the closing operation initiation instant onward, the *CBDS* curve can be modeled as an oblique line whose slope is equal to the *RDDS* with a negative sign [35].

Current begins to flow through the CB before the closing operation completes, thanks to the formation of an electric arc that establishes an electrical connection. The conductance is initiated at a so-called making instant (t_m), once the *CBDS*curve intersects the absolute gap voltage (the voltage across the CB poles) for the first time. The making instant associated with a given t_{ct} is the smallest t that satisfies the following equation

$$|v(t)| + s(t - t_{ct}) = 0 \tag{2}$$

where the quantity inside the absolute value symbol is the CB's instantaneous gap voltage and s is equal to *RDDS*.

The *RDDS* is not certain but can be assumed to vary within a known range $[s^{min}, s^{max}]$ with expected mean value s^{mean}. This uncertainty associated with the *RDDS* is commonly referred to as *RDDS* scatter. The closing time of a CB is not definite either and is typically assumed to spread over a range with length ΔT_{CB} and mean T_{CB}. This is normally referred to as mechanical scatter. Owing to the uncertainties just described, the *RDDS* and closing time are both indefinite and demonstrate probabilistic behavior in different closing attempts. The CB starts closing at a given instant but due to mechanical scatter, the contact touch does not take place at a certain instant. Instead, this instant spreads out in the range $[t_{ct} - \Delta T_{CB}, t_{ct} + \Delta T_{CB}]$.

Due to mechanical and *RDDS* scatter, making does not necessarily happen at the target making point, but at a range around it on the curve of absolute gap voltage. In Fig. 2, the target making point is denoted by q_m and the feasible making range is shown in red. As such, the true making instant might be slightly shifted to either side of t_m as the ideal target

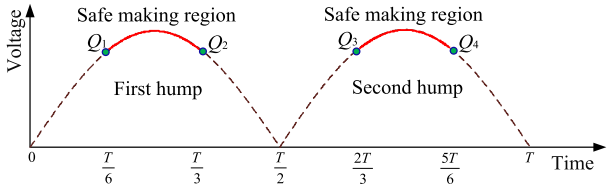

FIGURE 4. Safe making regions whose corresponding prospective flux can be equated by the residual flux density regardless of the core's material.

making instant. The true *CBDS* curve in an arbitrary closing attempt remains an oblique line in the shaded area shown in Fig. 2. The maximum positive and negative deviations from the target making instant correspond to s^{min} and $T_{CB} - \Delta T_{CB}$, and s^{max} and $T_{CB} + \Delta T_{CB}$, respectively, as demonstrated in Fig. 2. In this paper, *RDDS* and T_{CB} are assumed to have normal distributions around their mean (ideal) values. The standard deviation of each of these two random variables is reported based on the corresponding variation range and the 3-σ criterion [36]. Accounting for these uncertainties is key to ensuring a well-informed control switching stage, thus an energization with no to very little inrush current.

IV. PROPOSED METHOD

A V/V transformer contains two single-phase transformers known as the α-side and β-side transformers. Fig. 3 shows a typical traction power supply system with a V/V transformer, which is equipped with a railway power conditioner. The α-side and β-side transformers are magnetically decoupled, which means their cores are not connected. Hence, the residual flux of each of the two single-phase transformers can be adjusted independently. To flux the α-side and β-side transformers from the secondary side, each leg of the railway power conditioner can be controlled separately. The α- and *R*-legs can be used to flux the α-side transformer, and the β-side transformer is fluxed via the β-leg and *R*-leg. The *R*-leg is common between α-side and β-side transformers, and hence, its current is the opposite of the sum of α- and β-legs' currents.

This section proposes an effective method for adjusting the residual flux density of the α-side and β-side transformers to any given $B_r^{ad} \in [-0.5B^{max}, 0.5B^{max}]$, which is called the guaranteed range as will be explained in Subsection IV-A. The energization instant for each of the two transformers is then obtained so as to minimize the difference between B_r^{ad} and B_p. The operating characteristics and limitations of CBs are taken into account to establish a sound flux matching procedure capable of stopping inrush current from occurring.

A. CONTROLLED SWITCHING ON THE V/V TRANSFORMER

The first step in controlled switching is to obtain the voltage between the moving and fixed contacts of each CB pole when the CB is open. When all CB poles are open in Fig. 3, the gap voltages v_{ga}, v_{gb} and v_{gc}, are equal to the phase voltages u_a, u_b, and u_c, respectively. It can be easily confirmed that the gap voltages are not independent and change when any of the three poles is closed. For example, if pole *C* of the CB is closed, $v_{ga} = u_{ac}$, $v_{gb} = u_{bc}$, and $v_{gc} = 0$. Let us suppose that pole *C* is closed after poles *A* and *B*have been closed. This makes the voltages across the α-side and β-side windings jump immediately from u_{ab} and $-u_{ab}$ to u_{ac} and u_{bc}, respectively. The transformer's core may get saturated due to this sudden voltage change, which is not desirable. Hence, this paper suggests that pole *C* (the pole in the middle in Fig. 3) must get closed before the other two poles. This is to avoid any core saturation due to a sudden change in the windings' voltage.

With pole *C* closed and poles *A* and *B* open, v_{ga} and v_{gb} become equal to u_{ac} and u_{bc}, respectively. In this way, the gap voltages of the two transformers, i.e., v_{ac} and v_{bc}, will be identical but with 60° phase-angle displacement. Let us denote the fundamental frequency of the CB's gap voltage by f. The period of this voltage will be the reciprocal of the frequency as $T = \frac{1}{f}$. The absolute value of the CB's gap voltage is also a periodic function with period $\frac{1}{2f}$. Without loss of generality, the same making voltage can be aimed for energizing each of the α-side and β-side transformers. For this to happen, the time difference for energizing the two transformers should be $\frac{T}{6}$.

The maximum residual flux density of the core can take a value from 50% to 90% of B^{max}, depending on the core's material [37]. This means adjusting the absolute value of B_r to quantities greater than $0.5B^{max}$ may or may not be feasible. Conversely, a residual flux equal to or below $0.5B^{max}$ is almost always possible. To remove the need for any detailed information about the *B-H* characteristics of the core, this paper suggests taking $[-0.5B^{max}, 0.5B^{max}]$ as the guaranteed range for adjusting the residual flux within.

Fig. 4 shows part of the CB's absolute gap voltage, which is a sinusoidal hump that repeats at time intervals of $\frac{T}{2}$ (equivalent to an argument of π rad). A rising zero-crossing of the gap voltage is taken as the reference, i.e., $t = 0$. Here, our analysis is focused on the first and second humps. To energize during any other hump, it is sufficient to shift the timing of the actions by an appropriate multiple of the time constant T when following the steps outlined for the first or second hump. With reference to Q_1 and Q_2,the first hump can be divided into three regions; one from the origin to Q_1, another region from Q_1 to Q_2, and the third region from $Q_2$to the end of that hump. Similarly, the points Q_3 and Q_4 on the second hump also divide that hump into three different regions.

As per (1), making at the boundary points Q_1 or Q_2 results in $B_p = -0.5B^{max}$ or $B_p = 0.5B^{max}$, respectively. It can also be confirmed that making between Q_1 and Q_2 ensures that $-0.5B^{max} \leq B_p \leq 0.5B^{max}$. The region between Q_1 and Q_2 on the first hump of the absolute gap voltage, which is marked in red in Fig. 4, is of special importance to us and is called a safe making region. The safe region on the second hump lies between Q_3 and Q_4. The prospective flux density associated with a making anywhere in these safe regions can be equated by an identical residual flux density

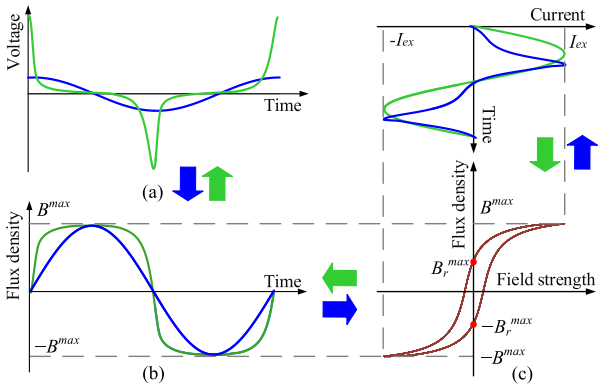

FIGURE 5. Transformer's (a) Winding voltage, (b) Core's flux density, (c) Current and *B-H* curve following Scenarios 1 and 2.

regardless of the transformer's core material. The same does not necessarily apply to making points, for example, on the first hump but outside the feasible region corresponding to $|B_p| > |0.5B^{max}|$. Similarly, whether the prospective flux of a making on the second hump (outside the safe marking region) can be equated by an identical residual flux density is uncertain and depends on the core material.

As mentioned earlier, making cannot be guaranteed to happen at a certain target time but a range around it, owing to *RDDS*and mechanical scatter. As discussed in [38], targeting points on the rising half of the absolute gap voltage results in a smaller making range around the target point. Thus, Q_1 can be considered an optimal target point for making in the safe region of the first hump. This will ideally result in energization at $t = \frac{T}{6}$ and a prospective flux of $B_p = -0.5B^{max}$. Aiming for Q_3 the second hump will ideally result in energization at $t = \frac{2T}{3}$ with prospective flux $B_p = 0.5B^{max}$.

Now, let us obtain the closing initiation and mechanical contact touch instants that correspond to making at Q_1 on the first hump. As per the time reference chosen in Fig. 4, $|V_m \sin(\omega t)|$ denotes the absolute gap voltage. First, mechanical and *RDDS* scatter is disregarded, and the prime sign is used to mark the corresponding instant of contact touch as t'_{ct}. With making voltage $\frac{\sqrt{3}V_m}{2}$ and $-s^{mean}$ as the slope of the *CBDS* curve, t'_{ct} can be obtained from

$$t'_{ct} = \frac{T}{6} + \frac{\sqrt{3}V_m}{2s^{mean}} \tag{3}$$

Equation (3) gives t'_{ct} with the assumption that there is no mechanical or *RDDS* scatter. In practice, however, the *RDDS*and closing time may vary slightly in different closing attempts, thereby resulting in a range instead of a certain making instant. This range might be even so wide that includes part of the previous sinusoidal hump. Making on a previous hump with an opposite voltage polarity could result in a considerable difference between the true and target prospective fluxes. Let us assume that t_{crit} demonstrates the earliest closing initiation instant that prohibits making on the previous hump even with extreme values for closing time and *RDDS*, i.e. s^{min} and $T_{CB} - \Delta T_{CB}$. To guarantee making happens on the first hump, the closing initiation instant must be obtained from

$$t_{in} = \max(t'_{ct} - T_{CB}, t_{crit}) \tag{4}$$

It can be easily confirmed that when $t'_{ct} - T_{CB} < t_{crit}$, the resulting t_m would be slightly greater than $\frac{T}{6}$. This conservative t_{in} ensures that making does not happen on the previous hump, while the target making remains the same or as close as possible to Q_1. In this case, t_m can be calculated by setting $s = s^{mean}$ and $t_{ct} = t_{in} + T_{CB}$ in (2). With the time reference of Fig. 4, energizing the transformer at t_m will result in

$$B_p = -B^{max}\cos(\omega t_m) \tag{5}$$

The next step is to adjust the core's residual flux to the value given by (5) and then energize the transformer at $t = t_m$. With pole C of the high voltage CB closed, the absolute gap voltages $|v_{ga}|$ and $|v_{gb}|$ will have $\frac{\pi}{3}$ rad phase displacement. If the β-side transformer is energized with a time delay of $\frac{T}{6}$ after the α-side transformer is energized, the prospective fluxes of the two transformers will have the same magnitude and sign. To take advantage of this, the residual flux density of the α-side and β-side transformers can be adjusted to the same value using the technique that will be explained in the next subsection. Then the two transformers are energized with $\frac{T}{6}$ time delay.

B. RESIDUAL FLUX ADJUSTMENT

The purpose of flux adjustment is to take advantage of the *B-H* characteristic to modify the core's residual flux density from an unknown initial value of B_r to a desired value of B_r^{ad}. It will be quite advantageous and sometimes even necessary if the flux adjustment process does not require the knowledge of the initial residual flux or the core's *B-H* characteristics. The subsection argues that current injection is the preferred method for adjusting residual flux density, as opposed to applying voltage to the winding. It is also shown that the amplitude of the excitation current is the only information needed to accomplish this. Then, a simple yet effective technique is presented for the estimation of the core's flux density over the course of the flux adjustment process.

1) VOLTAGE OR CURRENT CONTROL

By varying either the flux density or the magnetic field (B or H) in a controlled way, a given hysteresis loop can be traversed. Nevertheless, neither of these variables is directly accessible and they can only be indirectly controlled by changing voltage across and current injected into the transformer windings. This part explains how injecting appropriate sinusoidal current into the winding can adjust the residual flux to a credible reference value. It also discusses why applying sinusoidal voltage across the winding should be avoided, by highlighting complications this may introduce into the flux adjustment process.

Without loss of generality, let us consider a single-phase transformer with a unity turns-ratio. The nominal voltage

and amplitude of nominal excitation current (i.e., V_m and I_{ex}, respectively) are assumed to be known. No information about the nominal and inner hysteresis loops of the core (B-H characteristics) is assumed to be available. To begin our discussion, let us consider an easy case where the initial residual flux density of the core is zero ($B_r = 0T$). The nominal voltage $v(t) = V_m\cos(\omega t)$ shown in blue in Fig. 5(a) can be applied to the secondary winding while the primary winding is left open-circuited. This results in a sinusoidal flux density that varies in the range $[-B^{max}, B^{max}]$. Examining Fig. 5 in an anticlockwise direction and beginning with Fig. 5(a), one can observe how applying the nominal sinusoidal voltage to the secondary winding leads to the flow of a non-sinusoidal excitation current with amplitude I_{ex}. In the general case of non-zero initial flux density, however, applying nominal voltage to the transformer is not as convenient. This can saturate the core as per (1) and cause inrush current, which defeats the purpose of flux adjustment.

Now let us assume a sinusoidal current with amplitude I_{ex} is injected into the secondary winding. As a result, a non-sinusoidal voltage will be induced across the open-circuited primary winding, as indicated by examining Fig. 5 clockwise and starting at Fig. 5(c). The resulting flux density is not sinusoidal yet varies in the linear range $[-B^{max}, B^{max}]$. The flux density reaches $+B_r^{max}$ and $-B_r^{max}$ at falling and rising zero-crossings of the current waveform, respectively.

The magnetic field strength is assumed to be linearly proportional to the excitation current, while the flux density is a more complicated function of the voltage applied to the winding, as per (1). The coefficient and constant of this integral depend on the core parameters and original flux density, respectively. Without knowledge of this information, controlling the applied voltage to trace a given hysteresis loop would be difficult and time consuming. The initial flux density of the core could potentially cause an offset in the flux density. Such an asymmetry can easily saturate the core and push the magnetization of the core out of the nominal hysteresis loop.

The transition from the residual flux to the knee point for the first time is the only part of the magnetization that is influenced by the initial residual flux density, over the course of current injection. Once the knee point is reached, the subsequent trace of flux density becomes independent of the initial residual flux value. Thereafter, the trace is solely determined by the B-H characteristics of the transformer. At a zero-excitation current (while traversing the nominal hysteresis loop), the flux density is offset from the origin by the residual flux density $\pm B_r^{max}$. To be able to achieve smaller residual flux densities, inner hysteresis loops must be traversed. This can be achieved by injecting smaller sinusoidal current into the winding, as will be detailed in part 3 of this subsection.

2) FLUX DENSITY ESTIMATION

The transformer's flux density right at the de-energization instant may be estimated using two different approaches. One approach is to utilize (1), provided that N, A, B_r and the voltage applied are all known. An alternative approach is monitoring primary and secondary currents and voltages to track the core's magnetization along a hysteresis loop, if known. These two approaches require knowledge of the transformer's design information or the core's B-H characteristics. On the other hand, current and voltage measurements prior to the transformer disconnection may not be sufficiently accurate due to the transient responses of instrument transformers [34]. This is the case, for example, when the transformer disconnection has been caused by abnormal conditions such as a short-circuit fault. Once de-energized, the transformer's residual flux density begins to decline gradually through the CB grading capacitors and the stray capacitors of transformer bushings [30].

A simple technique is presented here to estimate the core's flux density relative to B^{max}, which will also be shown to be enough to enable the mitigation of inrush current. The sinusoidal alteration of H along the nominal hysteresis loop induces a voltage across the primary winding, which is not sinusoidal but periodic with the same period as that of the injected sinusoidal current. This is caused by the cyclic traversal of the closed hysteresis loop while the relationship between B and H is nonlinear. Let us assume $i_{inj}(t)$ is injected into the secondary winding at $t = 0$ and the induced voltage across the open-circuited primary winding of the transformer is measured. Let $T_r = 1/f_r$ denote the period of the injected sinusoidal current. The core flux density is a function of time and is shown by $B(t)$. It can be seen from Fig. 5 that $B(t)$ reaches its maximum, i.e., B^{max}, when $i_{inj}\left(\frac{T_r}{4}\right) = I_{ex}$. In its travel along the nominal hysteresis loop, $B(t)$ reaches $+B_r^{max}$, $-B^{max}$ and $-B_r^{max}$ when the injected current respectively reduces to zero and $-I_{ex}$ and then ascends to zero. These happen at $\frac{1}{2}T_r$, $\frac{3}{4}T_r$, and T_r, respectively.

Throughout the flux adjustment process, (1) in a more general form can be used to estimate the core's flux density at time t as below

$$B(t) = \frac{1}{NA}\int_0^t v(t)dt + B_r \tag{6}$$

In (6), the multiplier before the integral and B_r are unknown. The flux density at $\frac{T_r}{4}$ and $\frac{3T_r}{4}$ are respectively equal to B^{max} and $-B^{max}$, which can be examined using (6). The maximum and the initial residual flux densities (B^{max} and B_r) are unknown. Nevertheless, the integral term of (6) can be calculated using the terminal voltage, and can thus be considered known. In this way, a system of two equations in two unknowns can be formed and solved for the unknowns to arrive at

$$\begin{cases} B^{max} = \dfrac{1}{2NA}\left(\displaystyle\int_0^{\frac{T_r}{4}} v(t)dt - \int_0^{\frac{3T_r}{4}} v(t)dt\right) \\ B_r = \dfrac{-1}{2NA}\left(\displaystyle\int_0^{\frac{T_r}{4}} v(t)dt + \int_0^{\frac{3T_r}{4}} v(t)\,dt\right) \end{cases} \tag{7}$$

Let us use the hat sign to refer to the per-unit value of flux density. The per-unit value of $B(t)$, i.e., $\hat{B}(t)$, can be calculated

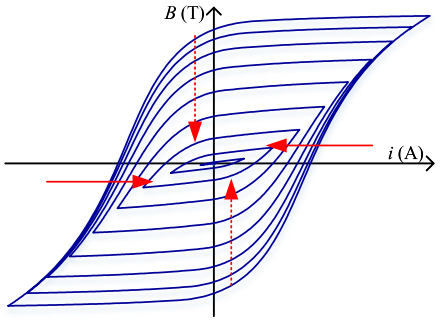

FIGURE 6. Moving inward through hysteresis loops by reducing the excitation current.

based on (6) and (7) as

$$\hat{B}(t) = \frac{B(t)}{B^{max}} = \frac{2\int_0^t v\,(t)\,dt - \int_0^{\frac{T_r}{4}} v\,(t)dt - \int_0^{\frac{3T_r}{4}} v\,(t)dt}{\int_0^{\frac{T_r}{4}} v\,(t)dt - \int_0^{\frac{3T_r}{4}} v\,(t)\,dt} \tag{8}$$

3) CURRENT INJECTION

For a successful flux adjustment, the frequency and amplitude of the injected current are both to be appropriately controlled. This current, denoted as $i_{inj}(t) = I_p \sin(2\pi f_r t)$, must be controlled to prevent core saturation, ensuring that I_p does not exceed I_{ex}. The amplitude of the injected current plays a key role in adjusting the residual flux density to any value within the range $\left[-B_r^{max}, B_r^{max}\right]$ rather than to its lower and upper bounds only.

The voltage induced across the primary winding by injecting current into the secondary winding is a function of the *B-H* curve and is also directly proportional to the rate of change of current based on Faraday's law [27]. Current of higher frequency may force the primary voltage to exceed the transformer's normal voltage. This means that a sinusoidal current with a larger f_r induces voltage with larger amplitude on the primary winding. This is in addition to the fact that at the same frequency, a current with a higher amplitude induces a higher voltage on the primary winding.

The amplitude of the injected current, i.e. I_p, is first set to I_{ex} to steer magnetization along the nominal hysteresis loop. An initial frequency of 1 Hz is adopted and then is increased in steps of 1 Hz at the end of each cycle. This is to increase the speed of the flux adjustment process by seeking a maximal yet safe frequency. To account for a safety margin, the frequency increment is continued until the amplitude of the induced voltage reaches 60% of the nominal voltage.

After fixing f_r, a current with amplitude $I_p = I_{ex}$ is injected for a full period. Removal of this current at $t = T_r$ adjusts the residual flux to $B_r^{ad} = B_r^{max}$. If the same current is continued to be injected for an extra half-cycle, $B_r^{ad} = -B_r^{max}$. Nevertheless, the (desired) reference residual flux might be lower than $\pm B_r^{max}$. The main idea here is to constantly alter the current amplitude to travel between inner hysteresis loops, as shown in Fig. 6. The current amplitude can gradually be decreased in order to move inward through inner hysteresis loops. This allows for reaching lower residual flux densities depending on the hysteresis loop being traversed. The red arrows in the figure show the direction of current reduction and the dotted red arrows signify the direction of residual flux reduction. A threshold can be set around the reference residual flux density to stop the current injection when the estimated residual flux density is within tolerance. In case the residual flux density exceeds the reference value by more than a certain percentage, the direction of change in current amplitude could be reversed at a lower rate to achieve the desired precision.

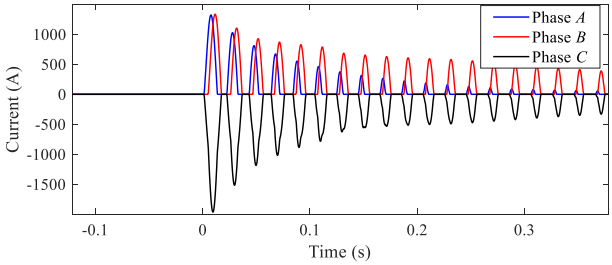

FIGURE 7. Inrush current drawn following the worst-case energization scenario.

TABLE 1. Parameters of the Jiles-Atherton model.

	α	a (A/m)	M_s (A/m)	k (A/m)	c
Type 1	2.5×10^{-5}	13.55	1.41×10^{6}	10	0.08
Type 2	2.5×10^{-5}	11.15	1.41×10^{6}	10	0.08

TABLE 2. Inrush Current Fallowing Casual Transformer Energizations.

Casual Energization Scenario	Current (A)					
	Core Type 1			*Core Type* 2		
	Min	Mean	Max	Min	Mean	Max
Random	7.39	761	1950.6	46.3	780	2283
Simultaneous	3.32	658.1	1922.6	0.61	688	2250
Pole-C First	0.518	721.6	1907.6	0.454	838.7	2277

V. PERFORMANCE EVALUATION

To evaluate the performance of the proposed method, the traction power supply system (connected to a 220-kV, 50-Hz power system) shown in Fig. 3 is simulated in PSCAD/EMTDC. This V/V transformer contains two 25-MVA, 220 kV/27.5 kV core-type single-phase transformers that are simulated based on the terminal duality method (TDM) [39]. The peak value of the primary side nominal current of the transformer is 160 A. The nonlinearity of the core is modeled using the inverse Jiles-Atherton model [40]. For single-phase transformers, B^{max} is set to 1.5 T. Two different cores with $B_r^{max} = 0.6B^{max}$ and $B_r^{max} = 0.75B^{max}$ are examined, which are referred to as *Type* 1 and *Type* 2, respectively. Table 1 lists the parameters used in the Jiles-Atherton model for these core types. The peak amplitude of excitation

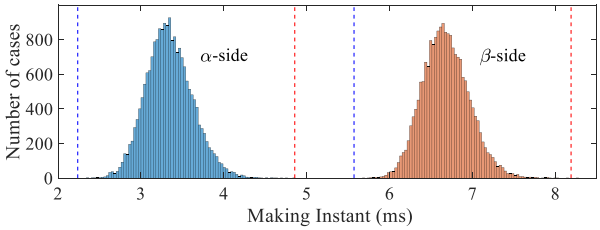

FIGURE 8. Distribution of the making instant for the α-side and β -side transformers.

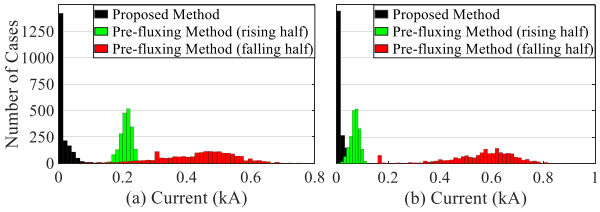

FIGURE 9. Distribution of inrush current amplitude upon V/V transformer energization of (a) Type 1 and (b) Type 2 transformers by different methods.

currents of *Type* 1 and *Type* 2 are 0.4 A and 0.3 A. A nine-level modular multilevel railway power conditioner (HB-MMC3 RPC [41]) with a DC link voltage of 41 kV is used as a current source for flux adjustment. The controls used on this HB-MMC3 RPC are as detailed in [42].

In what follows, first, three casual energization scenarios (random, simultaneous, and Pole-C first) are defined and studied in terms of resulting inrush currents. Next, the proposed method's capability to target Q_1 on the first hump of the gap voltage is analyzed. The proposed method, the pre-fluxing method [24], and the random energization method are then compared in Subsection V-C. The flux adjustment process for the V/V transformer is detailed in Subsection V-D, which is followed by the experimental validation results.

A. TRANSFORMER CASUAL ENERGIZATION

A casual energization scenario refers to switching sequences that are not aimed at removing inrush current. It goes without saying that the inrush current drawn following a casual energization scenario could become very large. First, let us consider an extreme case for core *Type* 1 where $B_r = B_r^{max} =$ 0.9T and the α-side and β-side transformers are energized at 0s and 3.3ms, which mark the rising zero-crossing of their corresponding gap voltages, respectively. Fig. 7 shows the inrush current drawn by the *Type* 1 V/V transformer following this energization scenario. The currents of phases A, B, and C reach 1.329 kA, 1.33 kA, and -1.96 kA, respectively. The current of phase A reduces to normal faster than the currents of phases $B$and C. The main reason for this is that v_{bc} is not sinusoidal at the energization instant due to the presence of the inrush current of the α-side transformer and its impact on v_c.

Table 2 summarizes the result of three casual energization scenarios, namely random, simultaneous, and phase-C-closed

TABLE 3. Performance of the proposed method with and without scatter.

RDDS	s^{min}	s^{mean}	s^{max}
Closing Time	$T_{CB} - \Delta T_{CB}$	T_{CB}	$T_{CB} + \Delta T_{CB}$
t_{ct} (ms)	7.7	8.7	9.7
t_m (ms)	2.4	3.3	4.5
$\hat{B}_p$ (pu)	-0.7291	-0.5	-0.131

scenarios. The highest values among the three phases are reported. In a random energization scenario, the three CB poles are all closed over an interval of 20 ms with a random uniform distribution. The second scenario is simultaneous energization where the closing operations of the CB poles are initiated simultaneously. The third scenario ensures that pole C is already closed for a long time before the other two poles are randomly closed within a 20-ms period. It should be noted that in all scenarios, $RDDS = 50\text{kV/ms}$ with $\pm 10\%$ scatter, and $T_{CB} = 40\text{ms}$ with $\pm 1\text{ms}$ mechanical scatter. To account for the probabilistic nature of the parameters, each casual energization scenario is repeated 1000 times. As expected, the three-phase currents are several times larger than the transformer's nominal current (which is 160 A). In addition to troubling protective relays, such undesirable high-magnitude current would reduce the transformer's lifetime.

B. GENERAL PERFORMANCE EVALUATION: PROPOSED METHOD

The method's performance is first evaluated assuming the CBs are ideal (without *RDDS* and mechanical scatter). This means $T_{CB} = 40\text{ms}$, and $RDDS = 50\frac{\text{kV}}{\text{ms}}$. The α-side and β-side transformers are energized at Q_1 on the first odd hump. As per (3), the closing initiation instants are obtained to be -31.3ms and -28ms. These correspond to contact touch instants 8.7ms and 12ms, respectively. Making ideally takes place at 3.3ms and 6.6ms and results in a prospective flux of $\hat{B}_p = -0.5\text{pu}$ for both transformers. This means with $B_r^{ad} = -0.5\text{pu}$, inrush current can be fully mitigated, and hence, the V/V transformer's energization merely results in the flow of excitation current.

As mentioned earlier, unintentional making on a previous hump can result in a large discrepancy between the true and target prospective fluxes. This is not a concern with a primary voltage of 220-kV and an *RDDS* of $s^{mean} \geq 25\text{kV/ms}$ with a maximum of 30% scatter. It can be shown that even with mechanical scatter of up to $\Delta T_{CB} = 1\text{ms}$, targeting Q_1 does not lead to making on the previous hump. Table 3 summarizes the impact of scatter on the energization of the α-side transformer with Q_1 as the target making point. Considering the non-idealities, making on the α-side transformer does not happen at 3.3ms, rather it happens within the range [2.3ms, 4.5ms]. The same range for the β-side transformer in milliseconds is [5.6, 7.8] which includes the ideal instant of $t = 6.6\text{ms}$.

To statistically evaluate the effect of scatter on t_m, a sensitivity analysis is carried out by conducting 10,000

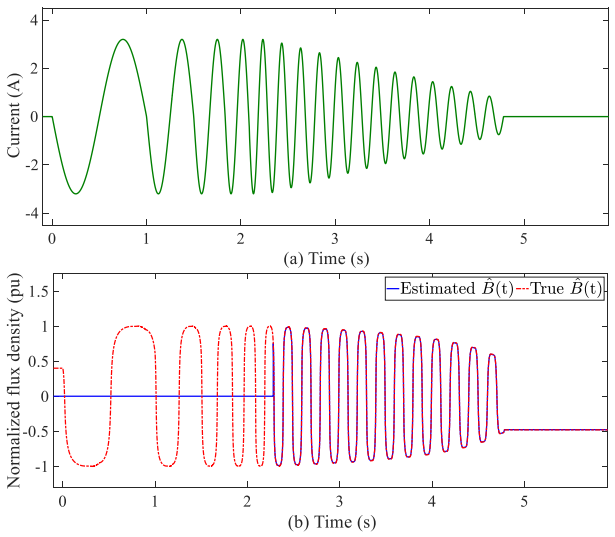

FIGURE 10. (a) Current injected into the secondary winding, and (b) true and estimated flux densities of the α-side transformer.

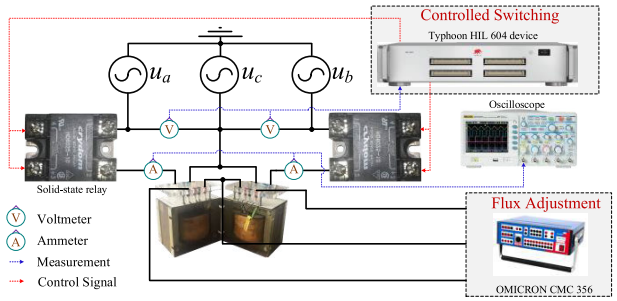

FIGURE 11. Test rig used to study different inrush current mitigating methods.

simulations. To account for the scatter, it is assumed that $\Delta T_{CB} = 1\text{ms}$ and $0.8s^{mean} < s < 1.2s^{mean}$. Fig. 8 shows the normal distribution of making instant for the a-side and β-side transformers. The target making instants, i.e., 3.3ms and 6.6ms, lie inside the area with the highest probability of occurrence. In most cases, a small difference exists between the true and target making instants.

C. COMPARISON WITH OTHER METHODS

The adjusted residual flux by the pre-fluxing method is either of the upper or the lower bound of the feasible range $[-B_r^{max}, B_r^{max}]$. The adjusted residual flux by the random energization method can take any value within this range. In this subsection, the proposed method is compared with the pre-fluxing method and the random energization scenario described in Subsection V-A. A total of 2,000 simulations are conducted to evaluate the performance of each method. The pre-fluxing method energizes the transformer at either the rising or falling halves of the absolute gap voltage. These target makings correspond to the prospective flux densities $-0.87B^{max}$ and $0.87B^{max}$, respectively. The adjusted residual flux densities by the proposed methods are assumed to be $B_r^{ad} = \pm 0.5B^{max}$. A uniformly distributed random error with upper and lower bounds of $\pm 5\%$ is considered for flux adjustment.

Figs. 9(a) and 9(b) demonstrate the distributions of inrush current of the V/V transformer by the proposed method and the pre-fluxing method targeting the rising and falling halves of the gap voltage. The outcome of random energization is not shown for it is almost evenly distributed from zero to the highest possible inrush current. The type of transformer core does not impact the performance of the proposed method. As shown, the method effectively limits the inrush current magnitude to 66% of the nominal current. The discrepancy between $0.87B^{max}$ and B_r^{max} is larger on the *Type*1 core than on the *Type* 2 core. Thus, the energization of *Type*1 by the pre-fluxing method results in a higher inrush current compared to that of *Type*2.

D. FLUX ADJUSTMENT

This subsection details the proposed residual flux adjustment procedure on the *Type*-1 core, as an example. The residual flux densities of the a-side and β-side transformers are assumed to be 0.6 T and -0.3 T, respectively. Taking B^{max} as the base flux density, the initial residual flux densities of the a-side and β-side transformers, and the maximum residual flux density of the core are 0.4, -0.2, and 0.6 pu, respectively. The injection of a sinusoidal current to the secondary winding with amplitude $I_{ex} = 3.2\text{A}$ is initiated at $t = 0$. The frequency of the injected current is maintained at 1Hz for a full cycle and is then continuously increased at the end of each cycle in 1-Hz steps. The voltage induced on the primary winding happens to exceed 60% of the nominal voltage when the frequency reaches 5Hz. Therefore at $t = 2.18\text{s}$,f_r is fixed at 5Hz to avoid any potential damage due to overvoltage.

Before targeting Q_1 on the first hump, it should be ensured that the residual flux is adjusted to -0.5 pu. Since this value is larger than B_r^{max} (-0.6 pu), the current amplitude is reduced at a rate of1A/s. The process will be stopped once the residual flux density lies within $\pm 5\%$ of the reference value -0.5 pu. Fig. 10(a) shows the injected current, and Fig. 10(b) shows the true/estimated flux densities of the a-side transformer's core in per unit. As can be seen from Fig. 10(a), the current injection is stopped at $t = 4.68\text{s}$ when the residual flux is adjusted to -0.48 pu, as depicted in Fig. 10(b).

The proposed flux adjustment approach is faster than that presented in [24]. To show this, *Type* 1 and *Type* 2 cores are considered. The proposed method is tested with reference values ranging from -0.66 pu to 0.66 pu. The initial residual flux of the core is assumed to have the maximum possible distance from the reference value. Results show that the proposed method does not take more than 10s for flux adjustment. Achieving the same using the pre-fluxing method needs a few minutes [24]. Speedy flux adjustment is in addition to the proposed method's ability to adjust the flux at any value within the feasible range. These have been achieved with no need for knowing any information about the B-H curve, which can be considered a great advantage.

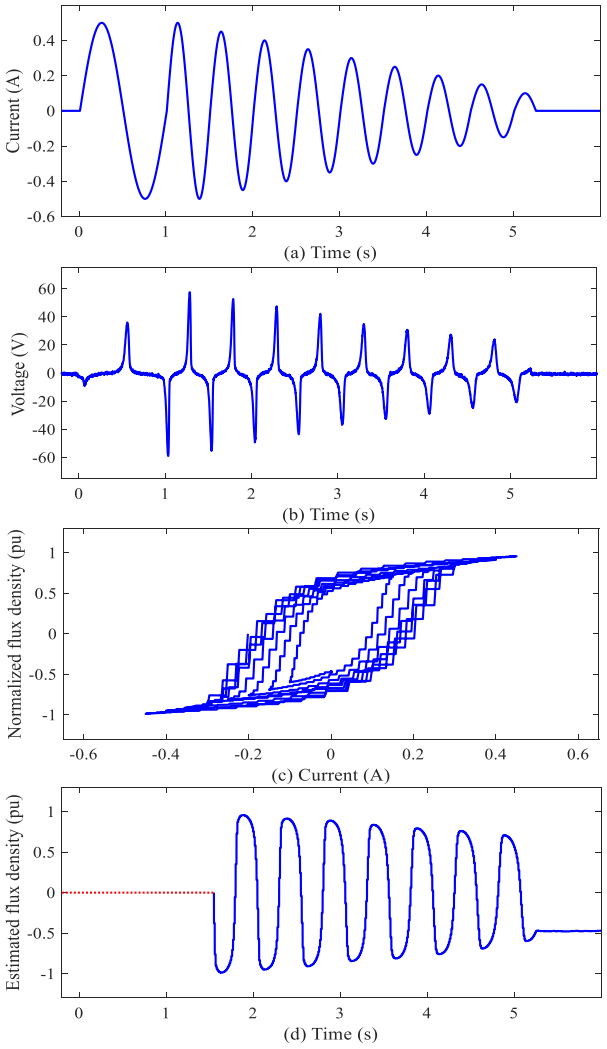

FIGURE 12. (a) Current injected into the secondary winding, (b) voltage induced on the primary winding of the α-side transformer, (c) B-H curve during current injection, and (d) estimated flux densities of the α-side transformer.

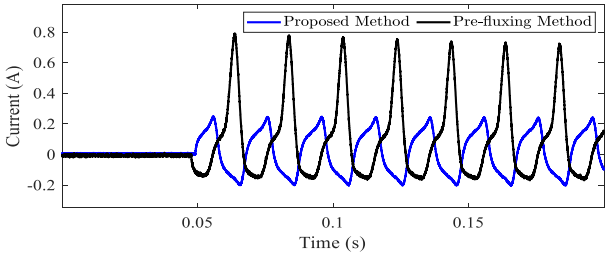

FIGURE 13. Inrush current drawn by the α-side transformer upon energization.

E. EXPERIMENTAL VERIFICATION

To demonstrate the effectiveness of the proposed method, a laboratory-scale V/V transformer is extensively tested on the test rig shown in Fig. 11. This V/V transformer is composed of two 400-VA, 260 V/120 V core-type single-phase transformers with $B_r^{max} = 0.78B^{max}$. The peak amplitude of the transformer's excitation current is 0.22 A. In the worst-case energization scenario, the current might increase as high as 50 A. An omicron CMC 356 relay tester is utilized as a current source for flux adjustment. The CB is modeled with an instantaneous turn-on solid-state relay controlled with a Typhoon HIL 604 device. All experimental results verify the obtained simulation results in the previous subsections.

An example of the flux adjustment process is shown in Fig. 12. At $t = 0$, a sinusoidal current with an amplitude of 0.5 A is injected into the secondary winding as shown in Fig. 12(a). At $t = 1.5$s, the frequency of the current waveform is fixed at 2Hz to avoid overvoltage in windings. As depicted in Fig. 12(b), the voltage is limited to 60 V, which is a safe voltage for the transformer. The current amplitude is then gradually reduced at a rate of 0.1 A/s to traverse inner *B-H* loops, as shown in Fig. 12(c). The injection process is set to stop when the residual flux density lies within $\pm 5\%$ of the reference value of -0.5 pu. According to Figs. 12(a) and 12(d), the injection process is stopped at $t = 5.26$s when the residual flux reaches -0.46 pu. Fig. 12(d) distinguishes two periods; the red part of the graph corresponds to the period before the frequency of the injected current is fixed when the flux density is not estimated. The blue part of the graph corresponds to the period after the frequency of the injected current is fixed when the flux density begins to be estimated. Finally, Fig. 13 demonstrates the current drawn by the transformer following its energization by the proposed and pre-fluxing methods. Using the proposed method, the current is limited to 250 mA, which is nearly equal to the transformer's excitation current. On the other hand, the inrush current reaches 800 mA by the pre-fluxing method. This 68% reduction in inrush current demonstrates that the proposed method outperforms the pre-fluxing method, even for transformers with high B_r^{max} values.

VI. CONCLUSION

This paper proposes a flux matching method to mitigate the inrush current of V/V traction transformers upon energization. The feasible range for adjusting residual flux is derived and an effective technique is proposed for achieving any desirable values in this range, as per the energization requirements. This is in contrast with previous methods that can only adjust the residual flux only at a few certain values such that the difference between residual and prospective fluxes is minimized. The proposed method determines a suitable making instant for energization considering the CB operating characteristics and scatter. The closing initiation instant is chosen in a way that ensures the difference between the prospective and adjusted flux density is minimal. This successfully mitigates the flow of inrush current without resorting to impractical tools and/or unrealistic assumptions.

The results of extensive simulations and experiments conducted confirm that the proposed method functions properly regardless of the transformer's core material and its initial flux density. It is also shown that the method is robust against a wide range of uncertainties emanating from *RDDS* and mechanical scatter. The method is shown to be able to limit

the magnitude of inrush current to 66% of nominal current, which can be considered a great leap forward in the face of all uncertainties involved. This is while with the pre-fluxing method, inrush current may exceed several times the nominal current, depending on the circumstances. The experimental results confirm the method's effectiveness in realistic conditions and its superiority over the pre-fluxing method.

REFERENCES

[1] S. E. Zirka, D. Albert, Y. I. Moroz, and H. Renner, "Further improvements in topological transformer model covering core saturation," *IEEE Access*, vol. 10, pp. 64018–64027, 2022.

[2] Z. Lihua, L. Jingjing, Y. Qingxin, Z. Jianguo, and C.-S. Koh, "An improved magnetostriction model for electrical steel sheet based on Jiles–Atherton model," *IEEE Trans. Magn.*, vol. 56, no. 3, pp. 1–4, Mar. 2020.

[3] C. Zhang, W. Ge, Y. Xie, and Y. Li, "Comprehensive analysis of winding electromagnetic force and deformation during no-load closing and short-circuiting of power transformers," *IEEE Access*, vol. 9, pp. 73335–73345, 2021.

[4] M. Tajdinian, H. Samet, and Z. M. Ali, "Differential protection algorithm founded on Kalman filter-based phase tracking," *IEEE Trans. Instrum. Meas.*, vol. 71, pp. 1–9, 2022.

[5] P. Mishra, A. Swain, A. Kumar Pradhan, and P. Bajpai, "Sequence current-based inrush detection in high-permeability core transformers," *IEEE Trans. Instrum. Meas.*, vol. 72, pp. 1–9, 2023.

[6] P. Liu, B. Jiao, P. Zhang, S. Du, J. Zhu, and Y. Song, "Countermeasure to prevent transformer differential protection from false operations," *IEEE Access*, vol. 11, pp. 45950–45960, 2023.

[7] V. Molcrette, J.-L. Kotny, J.-P. Swan, and J.-F. Brudny, "Reduction of inrush current in single-phase transformer using virtual air gap technique," *IEEE Trans. Magn.*, vol. 34, no. 4, pp. 1192–1194, Jul. 1998.

[8] J.-F. Chen, T.-J. Liang, C.-K. Cheng, S.-D. Chen, R.-L. Lin, and W.-H. Yang, "Asymmetrical winding configuration to reduce inrush current with appropriate short-circuit current in transformer," *IEE Proc. Electr. Power Appl.*, vol. 152, no. 3, pp. 605–611, 2005.

[9] M. T. Hagh and M. Valizadeh, "Analysis and comparative study of transient inrush current reduction methods," in *Proc. Int. Power Eng. Conf. (IPEC)*, Dec. 2007, pp. 287–291.

[10] Y. Cui, S. G. Abdulsalam, S. Chen, and W. Xu, "A sequential phase energization technique for transformer inrush current reduction—Part I: Simulation and experimental results," *IEEE Trans. Power Del.*, vol. 20, no. 2, pp. 943–949, Apr. 2005.

[11] W. Xu, S. G. Abdulsalam, Y. Cui, and X. Liu, "A sequential phase energization technique for transformer inrush current reduction—Part II: Theoretical analysis and design guide," *IEEE Trans. Power Del.*, vol. 20, no. 2, pp. 950–957, Apr. 2005.

[12] M. Tarafdar Hagh and M. Abapour, "DC reactor type transformer inrush current limiter," *IET Electr. Power Appl.*, vol. 1, no. 5, pp. 808–814, 2007.

[13] H.-T. Tseng and J.-F. Chen, "Voltage compensation-type inrush current limiter for reducing power transformer inrush current," *IET Electr. Power Appl.*, vol. 6, no. 2, pp. 101–110, 2012.

[14] H.-C. Seo, C.-H. Kim, S.-B. Rhee, J.-C. Kim, and O.-B. Hyun, "Superconducting fault current limiter application for reduction of the transformer inrush current: A decision scheme of the optimal insertion resistance," *IEEE Trans. Appl. Supercond.*, vol. 20, no. 4, pp. 2255–2264, Aug. 2010.

[15] A. Ketabi and A. R. H. Zavareh, "New method for inrush current mitigation using series voltage-source PWM converter for three phase transformer," in *Proc. 2nd Power Electron., Drive Syst. Technol. Conf.*, Feb. 2011, pp. 501–506.

[16] R. Cano-González, A. Bachiller-Soler, J. A. Rosendo-Macías, and G. Álvarez-Cordero, "Controlled switching strategies for transformer inrush current reduction: A comparative study," *Electr. Power Syst. Res.*, vol. 145, pp. 12–18, Apr. 2017.

[17] J. H. Brunke and K. J. Frohlich, "Elimination of transformer inrush currents by controlled switching. I. Theoretical considerations," *IEEE Trans. Power Del.*, vol. 16, no. 2, pp. 276–280, Apr. 2001.

[18] J. H. Brunke and K. J. Frohlich, "Elimination of transformer inrush currents by controlled switching. II. Application and performance considerations," *IEEE Trans. Power Del.*, vol. 16, no. 2, pp. 281–285, Apr. 2001.

[19] X. Lin, J. Zhang, J. Xu, J. Zhong, Y. Song, and Y. Zhang, "Dynamic dielectric strength of C_3F_7CN/CO_2 and C_3F_7CN/N_2 gas mixtures in high voltage circuit breakers," *IEEE Trans. Power Del.*, vol. 37, no. 5, pp. 4032–4041, Oct. 2022.

[20] M. A. Atefi and M. Sanaye-Pasand, "Improving controlled closing to reduce transients in HV transmission lines and circuit breakers," *IEEE Trans. Power Del.*, vol. 28, no. 2, pp. 733–741, Apr. 2013.

[21] *Controlled Switching, Buyer's and Application Guide*, A. J. A. L. Brochure, Schweden, U.K., 2010.

[22] C. Huo, S. Wu, Y. Yang, C. Liu, and Y. Wang, "Residual flux density measurement method of single-phase transformer core based on time constant," *IEEE Access*, vol. 8, pp. 171479–171488, 2020.

[23] Z. Emin et al., "Transformer energization in power systems: A study guide," CIGRE, Paris, France, Tech. Rep. TB 568, 2014.

[24] D. I. Taylor, J. D. Law, B. K. Johnson, and N. Fischer, "Single-phase transformer inrush current reduction using prefluxing," *IEEE Trans. Power Del.*, vol. 27, no. 1, pp. 245–252, Jan. 2012.

[25] D. I. Taylor, "System, apparatus, and method for reducing inrush current in a three-phase transformer," U.S. Patent 8 878 391 B2, Nov. 4, 2014.

[26] Y. Pan, X. Yin, Z. Zhang, B. Liu, M. Wang, and X. Yin, "Three-phase transformer inrush current reduction strategy based on prefluxing and controlled switching," *IEEE Access*, vol. 9, pp. 38961–38978, 2021.

[27] S. J. Chapman, "Electric machinery fundamentals fifth edition," in *Electric Machinery Fundamentals*, 5th ed. New York, NY, USA: McGraw-Hill, 2012.

[28] H. Zhang, J. Long, X. Li, Y. Xu, J. Shi, L. Ren, W. Yang, Z. Wang, and M. Chen, "A new method to measure the residual flux by magnetic sensors and a finite-element model," *IEEE Trans. Instrum. Meas.*, vol. 72, pp. 1–10, 2023.

[29] J. Xu, C. Sun, and Y. Liu, "A new demagnetization method for traction transformer of multi system electric locomotive," in *Proc. IEEE Transp. Electrific. Conf. Expo, Asia–Pacific (ITEC Asia–Pacific)*, May 2019, pp. 1–6.

[30] *Guidelines and Best Practices for the Commissioning and Operation of Controlled Switching Projects*, document CWG3.35 389, 2019.

[31] A. Luo, C. Wu, J. Shen, Z. Shuai, and F. Ma, "Railway static power conditioners for high-speed train traction power supply systems using three-phase V/V transformers," *IEEE Trans. Power Electron.*, vol. 26, no. 10, pp. 2844–2856, Oct. 2011.

[32] P. Bimbhra and G. Garg, *Electrical Machines—I*. Khanna Publishing House, 2014.

[33] U. Parikh and B. R. Bhalja, "Mitigation of magnetic inrush current during controlled energization of coupled un-loaded power transformers in presence of residual flux without load side voltage measurements," *Int. J. Electr. Power Energy Syst.*, vol. 76, pp. 156–164, Mar. 2016.

[34] P. M. Anderson, C. F. Henville, R. Rifaat, B. Johnson, and S. Meliopoulos, *Power System Protection*. Hoboken, NJ, USA: Wiley, 2022.

[35] H. Hamada, A. Eto, T. Maekawa, T. Koshizuka, S. Nishiwaki, N. Miyake, K. Arai, and M. Kosakada, "RDDS (rate of decrease of dielectric strength) measurement for gas circuit breaker," in *Proc. IEEE/PES Transmiss. Distrib. Conf. Exhib.*, vol. 3, Oct. 2002, pp. 1755–1759.

[36] H. Ito, *Switching Equipment*. Springer, 2019.

[37] R. Hamilton, "Analysis of transformer inrush current and comparison of harmonic restraint methods in transformer protection," *IEEE Trans. Ind. Appl.*, vol. 49, no. 4, pp. 1890–1899, Jul. 2013.

[38] U. Parikh and B. R. Bhalja, "Challenges in field implementation of controlled energization for various equipment loads with circuit breakers considering diversified dielectric and mechanical characteristics," *Int. J. Electr. Power Energy Syst.*, vol. 87, pp. 99–108, May 2017.

[39] C. Alvarez-Marino, F. de Leon, and X. M. Lopez-Fernandez, "Equivalent circuit for the leakage inductance of multiwinding transformers: Unification of terminal and duality models," *IEEE Trans. Power Del.*, vol. 27, no. 1, pp. 353–361, Jan. 2012.

[40] R. Naghizadeh, B. Vahidi, and S. Hosseinian, "Modelling of inrush current in transformers using inverse Jiles–Atherton hysteresis model with a neuro-shuffled frog-leaping algorithm approach," *IET Electr. Power Appl.*, vol. 6, no. 9, pp. 727–734, 2012.

[41] S. Song, J. Liu, S. Ouyang, and X. Chen, "A modular multilevel converter based railway power conditioner for power balance and harmonic compensation in Scott railway traction system," in *Proc. IEEE 8th Int. Power Electron. Motion Control Conf. (IPEMC-ECCE Asia)*, May 2016, pp. 2412–2416.

[42] M. Hagiwara and H. Akagi, "Control and experiment of pulsewidth-modulated modular multilevel converters," *IEEE Trans. Power Electron.*, vol. 24, no. 7, pp. 1737–1746, Jul. 2009.

AMIR AGHAZADEH (Student Member, IEEE) was born in Tehran, Iran. He received the B.S. degree in electrical engineering from the Sadra Institute of Higher Education, Tehran, in 2010, and the M.S. degree in electrical engineering from the Amirkabir University of Technology (AUT), Tehran, in 2014. He is currently pursuing the Ph.D. degree in electrical engineering with the School of Electronic and Electrical Engineering, University of Leeds, Leeds, U.K. In 2013, he has established the Golden Group (G2), AUT, working on emerging and selected topics in power electronics. His research interests include power electronics, its application in power systems, and high-speed railway power supply system protection and controls.

EHSAN HAJIPOUR (Member, IEEE) received the B.Sc., M.Sc., and Ph.D. degrees in electrical engineering from the Sharif University of Technology, Tehran, Iran, in 2008, 2010, and 2017, respectively. He is currently an Assistant Professor with the Department of Electrical Engineering, Sharif University of Technology. His current research interests include power system protection, power system automation and cybersecurity, and smart protection, operation, and planning.

KANG LI (Senior Member, IEEE) received the B.Sc. degree in industrial automation from Xiangtan University, Hunan, China, in 1989, the M.Sc. degree in control theory and applications from Harbin Institute of Technology, Harbin, China, in 1992, the Ph.D. degree in control theory and applications from Shanghai Jiaotong University, Shanghai, China, in 1995, and the D.Sc. degree in engineering from Queen's University Belfast, Belfast, U.K., in 2015.

From 1995 to 2002, he was a Research Fellow with Shanghai Jiaotong University, Delft University of Technology, and Queen's University Belfast. From 2002 to 2018, he was with the School of Electronics, Electrical Engineering and Computer Science, Queen's University Belfast, where he was a Lecturer, in 2002, a Senior Lecturer, in 2007, a Reader, in 2009, and a Chair Professor, in 2011. He currently holds the Chair of Smart Energy Systems with the University of Leeds, Leeds, U.K. His research interests include nonlinear system modeling, identification, and control, and artificial intelligence, with applications to energy and power systems, smart grids, electric vehicles, electrification of railway systems, and energy management in energy-intensive manufacturing processes.

SADEGH AZIZI (Senior Member, IEEE) received the B.Sc. degree in electrical power engineering from the K. N. Toosi University of Technology, Tehran, Iran, in 2007, the M.Sc. degree in electrical power engineering from the Sharif University of Technology, Tehran, in 2010, and the Ph.D. degree in electrical power engineering from the University of Tehran, Tehran, in 2016. From June 2016 to January 2019, he was with The University of Manchester, Manchester, U.K., as a Postdoctoral Researcher, leading their work on the protection work package of the EU H2020 MIGRATE Project, in collaboration with more than 20 European transmission system operators and research institutes. He was with the Energy and System Study Center, Monenco Iran Consulting Engineers Company, Tehran, from 2009 to 2011, and Iran Grid Management Company, Tehran, from 2013 to 2016. He is currently a Lecturer of smart energy systems with the School of Electronic and Electrical Engineering, University of Leeds, Leeds, U.K. He is also a Task Leader of Cigré WG B5.57, which is investigating new challenges of frequency protection in modern power systems. His research interests include wide-area monitoring, protection and control systems, digital protective relays, and applications of power electronics in power systems. He is an Associate Editor of the *International Journal of Electrical Power and Energy Systems*.